Palatal rugae positional changes during orthodontic treatment of growing patients

Caroline Pazera[1], Nikolaos Gkantidis[1]

[1]Department of Orthodontics and Dentofacial Orthopedics, University of Bern, CH-3010, Bern, Switzerland

Running title: Rugae changes during orthodontic treatment

First author

Caroline Pazera, Department of Orthodontics and Dentofacial Orthopedics, University of Bern, Freiburgstrasse 7, CH-3010, Bern, Email: karo.p07@gmail.com

***Corresponding Author**

Nikolaos Gkantidis, Department of Orthodontics and Dentofacial Orthopedics, University of Bern, CH-3010, Freiburgstrasse 7, Bern, Switzerland

Tel.: +41 (0) 31 632 25 92, Fax: +41 (0) 31 632 98 69

Email: nikolaos.gkantidis@zmk.unibe.ch; nikosgant@yahoo.gr

Acknowledgements

We are very grateful to all the good colleagues who contributed to the collection of this patient sample. We also thank Prof. D. J. Halazonetis for his valuable comments on an earlier draft of this manuscript.

Palatal rugae positional changes during orthodontic treatment of growing patients

Abstract

Objectives: To investigate the anteroposterior and vertical changes of the median rugae area, which is commonly used as dental model superimposition reference, relevant to its underlying skeletal structures.

Settings and sample population: Retrospectively collected pre- and post-treatment cephalometric radiographs and 3D digital dental models of 24 orthodontic patients (age at treatment start: 12.26 ± 0.83 years; assessment period: 2.13 ± 0.68 years) were analysed. All had mild to moderate malocclusions that were treated non-extraction with full fixed appliances.

Material and Methods: The incisive papilla and rugae points were placed on the dental models that were then registered to the cephalometric radiographs. Afterwards, the radiographs were superimposed on Sella, ANS-PNS, and through a maxillary structural method. The vertical and horizontal movements of the papilla and the rugae points, as well as of a central incisor, were measured (Viewbox 4 software).

Results: The incisive papilla and the three rugae points remained stable anteroposteriorly, but moved downwards in the vertical dimension (approximately 1-2 mm), in a similar manner ($P>0.05$). However, the anteroposterior position of the papilla and the first rugae points were affected by changes in anterior tooth position and inclination ($p<0.05$).

Conclusion: Both the second and third rugae can be used as superimposition references for tooth movement assessment. The use of the papilla and the first rugae area is not recommended, because they are affected by tooth movement. The outcomes of a palatal superimposition are comparable to those of a maxillary skeletal superimposition in the anteroposterior, but not in the vertical dimension.

Keywords: digital dental model; cephalometric superimposition; three-dimensional superimposition; palatal rugae

Introduction

Researchers and clinicians have always been interested in assessing morphological changes due to treatment, growth, or pathology over time. Superimposition of serial patient images, primarily lateral cephalometric radiographs, has been widely used for this purpose (1, 2). However, the inherent limitations of this image type, attributed primarily to the fact that it depicts a 3D object in 2D, might add confusion to the outcomes (3). 3D superimposition techniques have been developed to overcome these shortcomings (4, 5). Even so, an inevitable limitation of any radiographic image concerns the patient risks originating from radiation exposure.

Recently, rapid advances in intraoral imaging technology enabled the creation of 3D intraoral surface models (6, 7). These models are obtained through a risk-free, convenient process and are relatively easy to use. Currently - with certain limitations - intraoral scanners have been shown to provide adequate image quality (7), which is an essential precondition for valid superimposition of serial models (8).

As in the case of radiographic data (4, 5, 9), a prerequisite for efficient intraoral model registration is the use of reference structures that are easily identified and remain morphologically stable over time. Several techniques have been used to superimpose serial 3D intraoral surface models. So far, there is no reliable area for mandibular 3D surface model superimposition (6). On the contrary, maxillary 3D surface model superimpositions have attracted more attention, showing promising results (6, 10). Most of the currently available techniques use the palatal rugae area as superimposition reference (6).

Thus, the morphological stability of the rugae area is crucial for the proper application of these 3D superimposition methods. In the literature, the rugae area (11, 12), and particularly the third rugae area, has been suggested as a stable structure (13-15), also during growth (10, 16, 17). However, most of the above studies assessed only differences in mean values, which might be misleading for diagnostic accuracy studies (18). Furthermore, there is high heterogeneity among existing studies in methodologies and outcomes, including participants' age, interventions (e.g. extraction or non-extraction cases), time lapse between serial models, and assessment methods.

No previous study assessed the spatial stability of the rugae according to the maxillary skeletal structures, concerning growing patients that were treated non-extraction, with fixed appliances. Nevertheless, this comprises the most common type of orthodontic treatment. Thus, our aim was to assess the anteroposterior and vertical stability of the rugae area relative to its skeletal basis, in a typical orthodontic patient sample, using 3D digital dental models and cephalometric radiographs. The null hypothesis of the study was that there is no difference in the stability of the three palatal rugae and the incisive papilla. The findings will facilitate the selection of proper dental model superimposition reference areas and the correct interpretation of the outcomes.

Materials and Methods

Ethical approval

The study protocol was approved by the Ethics Commission of the Canton of Bern, Switzerland (P roject-ID: 2019-00326) and by the Institutional Ethics and Research Committee of the 251 Hellenic Airforce Hospital, Athens, Greece (approval number: 076/10571/16.06.2018). The methods were carried out in accordance with the relevant guidelines and regulations. All participants signed an informed consent prior to the use of their data.

Sample

The sample consisted of pre- (T0) and post-orthodontic (T1) treatment cephalometric radiographs, and 3D dental models of 24 growing patients (7 males, 17 females; mean age at treatment start: 12.26 ± 0.83 years old; T0-T1 period: 2.13 ± 0.68 years), retrospectively selected from the archives of the Department of Orthodontics and Dentofacial Orthopedics, University of Bern, Switzerland and of two private clinics, in Switzerland and Greece. The following inclusion criteria were applied: a) European ancestry, b) no congenital anomalies, syndromes, or systemic diseases, c) non-extraction orthodontic treatment with fixed appliances in both jaws, d) 10.0 - 13.5 years old at treatment start (T0), e) treatment duration between 1.5 and 3.5 years, f) no appliance on the palate at least 1 year prior to T0 records and during treatment, g) early permanent dentition at T0, h) no missing teeth from 2nd molar to 2nd molar, i) no extreme malocclusion and craniofacial pattern at T0, j) molar Class I or less than ½ cusp Class II at T0, k) no severe posterior crossbite at T0, l) clinically acceptable occlusion at T1, m) cephalometric radiographs of adequate quality, with a ruler to measure the magnification factor, and n) cephalometric radiographs where both maxillary central incisors had similar position and inclination or where the right or left incisor was clearly visualized. More detailed description of all inclusion criteria is provided in Supplementary Table 1.

A search of consecutive patient files was applied to identify eligible patients. Sample size was based on a previous relevant study (14), where statistically significant results were obtained using a sample of 10 patients. To increase the power of our study we included 24 patients, based on availability of eligible records. For comparative statistics, post hoc power analyses revealed adequate power (power: 80%, a = 0.05) to detect a difference of 0.93 mm between the vertical movements of the second and the third rugae, and a 1.27 mm difference between the anteroposterior movements (G*power, version 3.1.9.4).

The 3D digital dental models originated from conventional dental casts obtained through alginate impressions, which were poured with plaster on the same day when the impression was taken. Each cast was scanned with a high accuracy laboratory 3D surface scanner (stripe light/LED illumination; accuracy <20 µm; Laboratory scanner D104a, Cendres + Métaux SA, Rue de Boujean 122, CH-2501 Biel/Bienne) to provide the required STL files for the study.

The cephalometric radiographs that were not in digital form were scanned at 300 dpi to be transformed to .jpeg files.

Digitization of cephalometric radiographs and Superimposition workflow

3D pretreatment (T0) and posttreatment (T1) dental models, as well as T0 and T1 cephalometric radiographs, were imported in Viewbox 4 software (version 4.1.0.1 BETA, dHAL, Software, Kiffissia, Greece) for further processing.

Various cephalometric landmarks (Supplementary Table 2) were placed on the cephalometric radiographs in the x-ray mode of the program. Additionally, to place the incisive papilla (P0) and the midpoints of the lines connecting the medial ends of each rugae (R1, R2, R3) (Figure 1) on the cephalometric radiographs, the corresponding 3D dental models were registered on the radiographs (Figure 2; Supplementary Table 2). Each 3D model was adjusted to be registered with the corresponding cephalometric radiograph through a manual best fit. This was performed at the 3D view of the software, according to a central incisor crown that was clearly depicted on the cephalometric radiograph, as well as the first molar crowns and the midline palatal curve (Figure 2B). Thus, the orientation of the 3D model in all three axes of space was considered for the registration with the cephalometric radiograph.

Once the landmark placement was completed, the radiographs, as well as all landmark, plane, and curve configurations were adjusted to real size, through a reference ruler depicted on each radiographic image.

Finally, the pterygomaxillary fissure point (PTM structural; Supplementary Table 2; Figure 2C) was placed on the T0 cephalometric radiograph and then transferred on the T1, following a maxillary structural superimposition. This was performed through a manual best fit of the images on the anterior zygomatic process, as defined by Björk and Skieller (1977) (2), but also taking into account the anterior wall of the pterygomaxillary fossa and other minor anatomical structures, in-between the above mentioned structures. To enhance this superimposition, a filter that adjusts the brightness and contrast was applied to the radiographic images, to better visualize the skeletal structures (Adaptive Auto Levels). Then, the T0 radiograph was colored in red and the T1 in green. The T0 radiograph was made transparent using the blending function of the software to enable the superimposition. The superimposition was performed by changing the position of the T0 image over the T1, until a maximum overlapping of the structures of interest, indicated by yellow colour, was achieved (Figure 3).

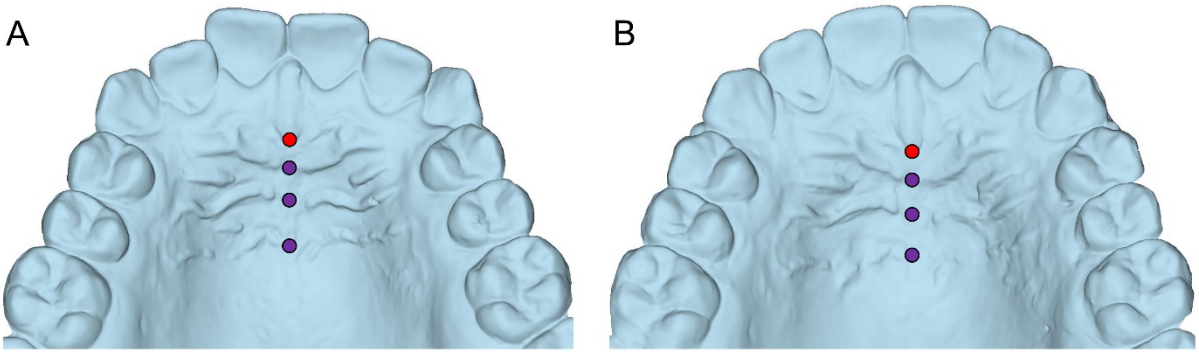

Figure 1. A. Pre-treatment and B. post-treatment maxillary dental models showing the landmarks placed in the palate to depict the distal point of the incisive papilla (P0; red circle) and the midpoints of the first, second, and third rugae, starting from mesially towards distally (R1, R2, R3; purple circles).

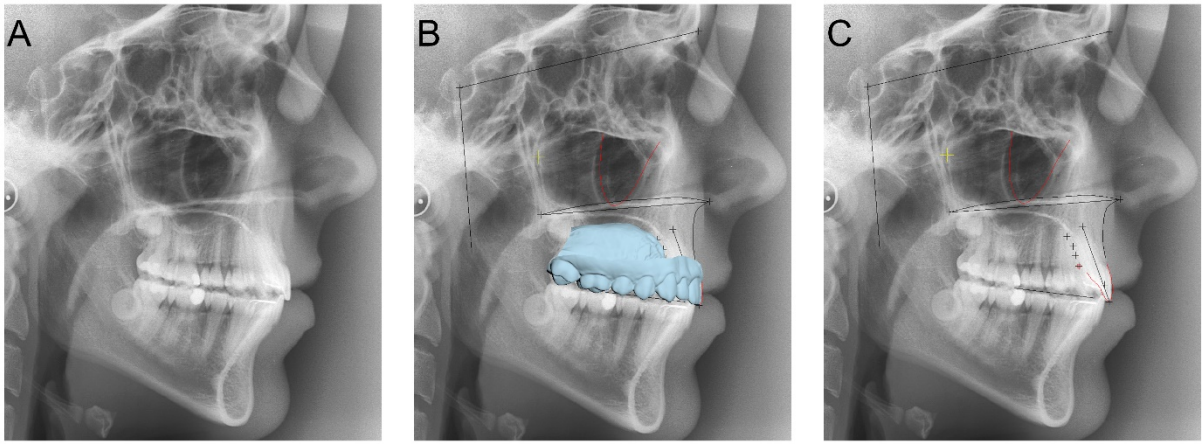

Figure 2. A. Post-treatment cephalometric radiograph. B. Post-treatment maxillary dental cast, registered on the corresponding cephalometric radiograph to facilitate the placement of the papilla and rugae points. C. All reference planes, curves, and landmarks placed on the cephalometric radiograph for the needs of the study. Detailed description is provided in Supplementary Table 2.

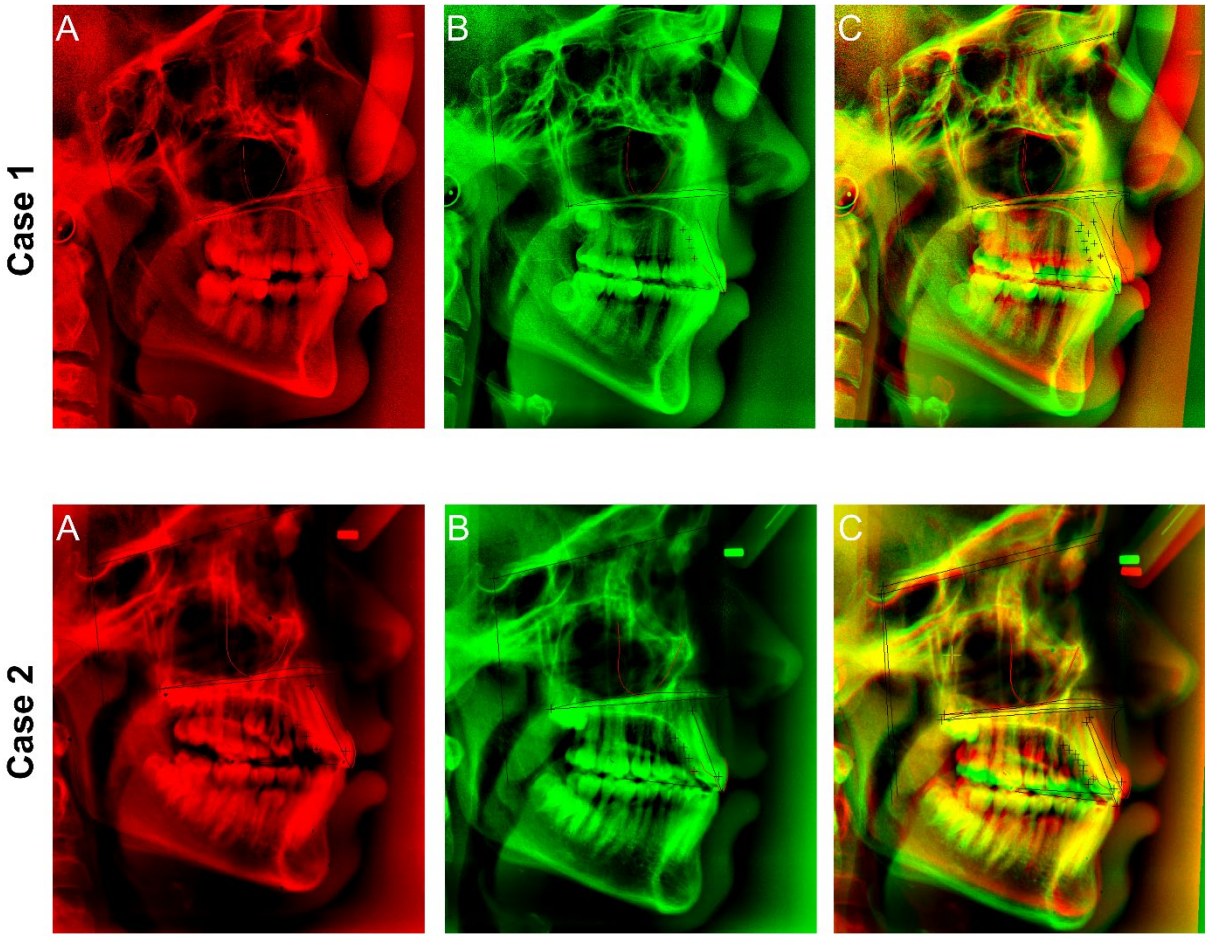

Figure 3. A. Pre-treatment and B. post-treatment cephalometric radiographs digitized and adjusted to facilitate the maxillary structural superimposition. C. Superimposed pre-and post-treatment radiographs. Yellow color indicates overlap of corresponding anatomical structures.

Measured outcomes

Measurements were performed through Viewbox 4 software, based on a predefined protocol.

The vertical movements of the papilla and rugae points were measured through:

1. T1-T0 differences in the vertical distance of each point from the ANS-PNS line.

2. T1-T0 differences in the vertical distance of each point from a line that is parallel to ANS-PNS and passes through the PTM structural point, placed following the maxillary structural superimposition.

The anteroposterior movements of the papilla and rugae points were measured as follows:

1. T1-T0 differences in the vertical distance of each point from a line that passes through Sella and is vertical to ANS-PNS. This measurement provides the movement of each point according to the cranial base, with maxillary growth incorporated to the outcome.

2. T1-T0 differences in the vertical distance of each point from a line which passes through PTM structural point and is vertical to ANS-PNS, following the maxillary structural superimposition.

The vertical and anteroposterior movement of the crown centroid (19), as well as the inclination change, of a specific central incisor that was easily identifiable in both cephalometric radiographs, were also measured. These measurements were performed along or vertical to the occlusal plane and following the maxillary structural superimposition.

Subsequent to landmark placement and superimposition process, all data were exported directly from Viewbox software to a Microsoft Excel data sheet (Microsoft Corporation, Redmond WA, USA), according to a predefined software protocol, for further processing.

Method error

The whole landmark placement and superimposition process, including all measurements, was repeated by the same investigator in ten randomly selected cases, following a 1-month period.

Statistical analysis

Statistical analysis has been performed through SPSS Software (IBM SPSS Statistics for Windows, Version 25.0. Armonk, NY: IBM Corp.).

Data were tested through the Shapiro-Wilk test and certain variables were found to deviate from normality. Thus, non-parametric statistics were used for the study.

The differences among rugae movements, following each superimposition, were tested in an unpaired manner using Kruskal-Wallis test. In case of significant results, further pairwise comparisons between rugae were performed using the Mann-Whitney U test.

The effects of incisor movement and inclination on the position of the papilla and rugae points were tested through Spearman's correlations. For correlations with $p < 0.10$, scatter plots showing individual data are provided in Supplementary Figure 1.

In all cases, two-sided significance tests were carried out at an alpha level of 0.05. A Bonferroni correction was applied to the level of significance in case of pairwise a posteriori multiple comparison tests, to reduce the possibility of false positive results.

Table 1. Spearman's correlations of the incisor movements and inclinations with the movements of the papilla and rugae points.

		Incisor					
		Vertical mov.		Horizontal mov.		Inclination	
		r	p	r	p	r	p
Maxillary structural superimp.	P0 vertical mov.	-0.197	0.356	0.403	0.051[a]	-0.322	0.125
	R1 vertical mov.	-0.287	0.174	0.368	0.077[a]	-0.193	0.367
	R2 vertical mov.	-0.240	0.258	0.153	0.476	0.010	0.965
	R3 vertical mov.	-0.375	0.071[a]	0.249	0.240	-0.093	0.665
	P0 horizontal mov.	-0.116	0.591	**0.612**	**0.001**	**-0.513**	**0.010**
	R1 horizontal mov.	-0.126	0.559	**0.417**	**0.042**	-0.355	0.089[a]
	R2 horizontal mov.	0.070	0.747	0.077	0.721	-0.144	0.503
	R3 horizontal mov.	0.179	0.401	-0.037	0.864	0.033	0.880
ANS-PNS superimp.	P0 vertical mov.	-0.128	0.551	0.21	0.324	-0.299	0.155
	R1 vertical mov.	-0.151	0.481	0.216	0.310	-0.225	0.290
	R2 vertical mov.	-0.128	0.551	-0.046	0.830	-0.083	0.699
	R3 vertical mov.	-0.247	0.244	0.058	0.789	-0.178	0.404

Bold color indicates significant correlations ($p<0.05$)
[a]Correlations that were close, but did not reach the level of significance ($0.05<p<0.10$)
mov.: movement; superimp.: superimposition

Results

The null hypothesis was rejected. According to the maxillary structural superimposition, the median anteroposterior position of all rugae points and the papilla point remained stable. No significant differences were detected among the anteroposterior movements of the tested points (Figure 4A; p = 0.501). However, the anteroposterior movement of the incisor was correlated to the anteroposterior movements of the papilla (P0) and the first ruga (R1) point (r = 0.612, p = 0.001; r = 0.417, p = 0.042, respectively; Table 1, Supplementary Figure 1). Furthermore, although the average anteroposterior position of the incisors remained stable (median: 0.25 mm movement), they were proclined by 3.8 degrees (median: 1.7 degrees) (Figure 5). Taken together, the above findings suggest that the incisors' roots moved posteriorly affecting mostly the P0, but also the R1 point, which both showed small posterior movements (median: -0.5 and -0.25 mm, respectively). Negligible anteroposterior movements were observed for R2 and R3 points (Figure 4A). The incisor proclination, which resulted in posterior root movement, was correlated to a posterior movement of the P0 point (r = -0.513, p = 0.010). A similar tendency was observed for R1 point (r = -0.355, p = 0.089; Table 1; Supplementary Figure 1).

According to Sella, the three rugae and the papilla points moved slightly forward in a similar manner. P0 moved less, probably affected by the change in incisor inclination, though this finding was not statistically significant (p = 0.781; Figure 4A).

According to the maxillary structural (vertical line from PTM Structural to ANS-PNS) and to ANS-PNS superimpositions, all rugae and papilla points moved downwards to a similar extent ($p = 0.750$ and $p = 0.904$, respectively; Figure 4B).

Overall, there was no significant difference in the anteroposterior and vertical spatial stability of the rugae and the papilla points. However, the anteroposterior position of the papilla and the first rugae points were found to be significantly affected by changes in the anterior tooth position and inclination. There was also a tendency that the vertical movements of the papilla and the first rugae were affected by the anteroposterior movement of the incisors, though this did not reach significance ($r = 0.403$, $p = 0.051$; $r = -0.368$, $p = 0.077$, respectively; Table 1; Supplementary Figure 1).

There were no clear differences in the amount of variations observed, concerning the vertical and anteroposterior movements of the papilla and rugae points (Figure 4).

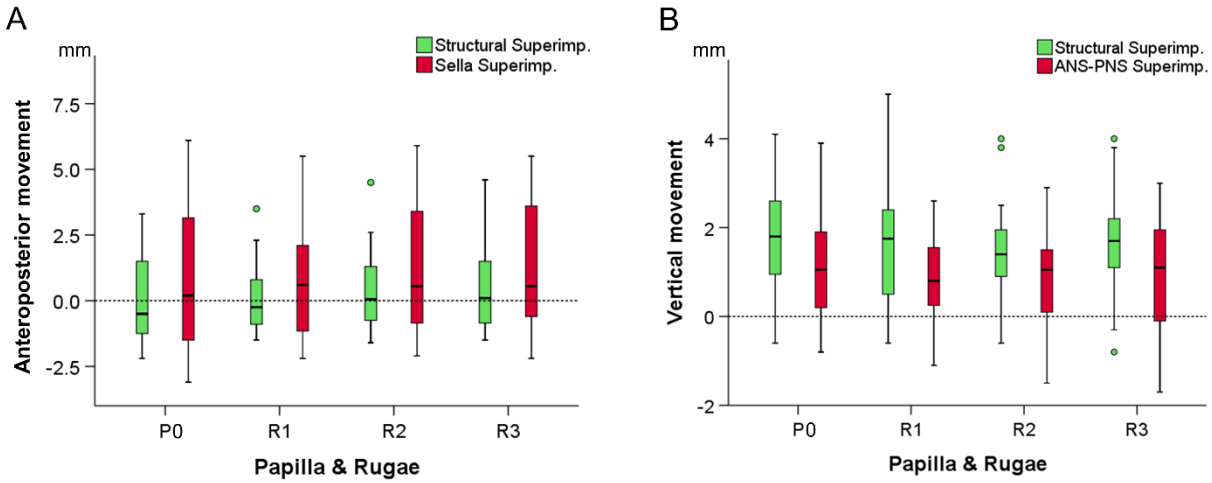

Figure 4. A. Box plots showing the anteroposterior movement of the papilla and rugae points during treatment, measured following the maxillary structural or the Sella superimposition of serial radiographs. B. Box plots showing the vertical movement of the papilla and rugae points during treatment, measured following the maxillary structural superimposition of serial radiographs or superimposition on ANS-PNS plane. The upper limit of the black line represents the maximum value, the lower limit the minimum value, the box the interquartile range, and the horizontal line the median value. Outliers are shown as colored dots. P0: papilla point; R1, R2, R3: rugae points.

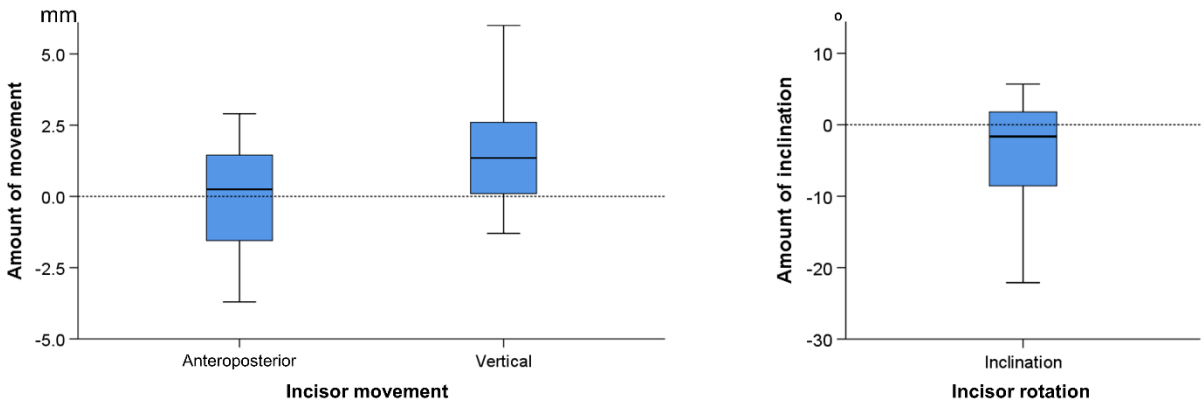

Figure 5. Box plots showing the anteroposterior and vertical movement, as well as the change in inclination due to treatment, of a central maxillary incisor, measured according to the occlusal plane, following the maxillary structural superimposition. The upper limit of the black line represents the maximum value, the lower limit the minimum value, the box the interquartile range, and the horizontal line the median value

Method error

The median error of all variables was 0.05 and ranged from -0.50 to 0.30 (° or mm, depending on the tested variable). The smallest difference between repeated individual measurements was -1.40 and the largest 1.70. When all differences between repeated measurements were transferred to absolute values, the median error was 0.35 and ranged from 0.15 to 0.90. These values refer to the overall error of landmark identification, as well as to the superimposition performance. Detailed information regarding the error of each single variable is provided in Supplementary Table 3.

Discussion

Currently, 3D dental model superimposition techniques are increasingly applied in daily practice due to the accurate, convenient, and radiation free model acquisition process. Such 3D techniques usually use the rugae area as superimposition reference (1, 6, 10). However, the accordance of the derived outcomes with those obtained from standard cephalometric superimposition techniques that use skeletal structures as references, remains largely unexplored. Our study is the first to assess the papilla and rugae points movements relative to the underlying maxillary skeletal structures, on a growing, orthodontically treated patient sample. This was achieved by registering 3D digital dental models on cephalometric radiographs and subsequently applying standard cephalometric superimposition techniques. Thus, the present results will facilitate the proper application and interpretation of intraoral 3D model superimposition techniques that use the rugae area as reference.

Overall, there were no significant differences in the anteroposterior and vertical movements of all papilla and rugae points during treatment. However, the papilla and the first rugae points were found to be affected by anterior tooth movement. Our results suggest that the closer to the teeth the higher the effect of tooth movement on the palatal structures. Thus, a maxillary model superimposition for tooth movement assessment is expected to provide more reliable outcomes when the papilla and the first rugae points are not included in the superimposition reference area. On the other hand, the second rugae area, which showed

similar changes to the third rugae area, can be included in the reference area, increasing in its size. A superimposition reference area of larger size has been shown to significantly restrict the effect of artifacts on the superimposition outcomes (8); thus providing more robust outcomes.

This consideration is of utmost importance, since artifacts are likely to be present in any type of model. In case of physical model construction, significant sources of artifacts comprise the flaws of the impression and stone model creation techniques (20). In physical models, surface artifacts typically occur in morphologically complex areas, such as the palatal rugae and are usually present in the form of small, bubble-type structures (8, 20). In case of intraoral digital model acquisition, artifacts might occur in areas with movable structures or in any other area, due to saliva or to interference of undesirable structures, during image acquisition. The inaccuracy of the digital model acquisition and creation process itself is also an artifact generating factor (7, 8).

According to the skeletal structures, the incisive papilla and the three rugae points remained stable anteroposteriorly during the tested period, but moved downwards in the vertical dimension (approximately 1-2 mm). Thus, the outcomes of a palatal rugae superimposition are comparable to those of a maxillary skeletal superimposition regarding the anteroposterior, but not the vertical dimension, where rugae movement over time should be considered.

We selected a sample with the specific malocclusion and age characteristics, because it may represent the most common type of orthodontic patient. The sample included growing patients, without severe malocclusion problems that were treated without tooth extractions. Growth was indicated by chronological age. No specific method was used to evaluate skeletal maturation stage, such as the cervical vertebrae method, since chronological age has been shown to provide similar level of information (21). The downward movement of the rugae points detected in our study, was expected due to the typical maxillary growth pattern, which includes bone apposition at the oral side of the palate and resorption at the nasal side. The forward movement of all rugae and papilla points following the Sella superimposition, is also in accordance with the maxillary growth pattern, which results to forward and downward movement of the maxilla, due to primary and secondary translation (22). Finally, the limited incisor movements are expected due to the tested malocclusion patterns and the relevant treatments.

We limited the malocclusion characteristics of the included subjects to obtain a robust sample. Although limited anterior tooth movements were evident in our sample, these were found to affect the papilla and first rugae points. However, the limited tooth movements might be the reason for not detecting any significant difference of the papilla and the first rugae from the second and third rugae point movements. In a sample with considerable anterior tooth movement, such differences might be evident. In the latter case, the papilla and the first rugae points would be expected to be highly affected by anterior tooth movement, but this remains to be tested.

Indeed, certain previous studies that tested premolar extraction cases showed that the first and second rugae are highly affected by incisor movements, in contrast to the third rugae (16, 17). Furthermore, a recent 3D dental model superimposition study on growing patients, treated for anterior crossbite, concluded that the medial part of the third rugae and a small area dorsal to it is a stable structure, since greater changes occurred in areas around the incisive papilla and the lateral parts of the palate (10). In another cephalometric superimposition study (14), where dental models were registered on cephalograms, significant differences were detected in the vertical rugae movements, suggesting that the median third rugae points are more stable. No differences were detected in anteroposterior rugae changes. However, this sample consisted of two groups of 10 adults and 13 late adolescents that were followed for a four-year period, after the end of orthodontic treatment. On the contrary to the above studies, Bailey et al., which measured distances between rugae points before and after treatment, in adult patients treated with, as well as without extractions, did not detect any clear difference (12). A similar conclusion was reported by Kim, who measured changes between rugae points in a longitudinal, untreated, growing sample (17). Finally, another study testing patients that underwent rapid maxillary expansion, followed by fixed appliance treatment, reported that the third rugae tended to show more changes due to palatal expansion than other rugae. The same study did not identify any difference between rugae point configurations in control, non-extraction patients, treated solely with fixed appliances (23). The conclusion of the latter studies is in agreement to our findings that the third rugae do not necessarily remain more stable compared to the other rugae, especially in patients treated with fixed appliances.

Overall, as suggested by the evidence discussed above and supported by the present findings, it seems that incisor movement is the key factor that determines the stability of the more anteriorly located rugae. Our results indicate that a potential difference in the stability of the rugae points might have not been detected due to the effects of incisor movement and inclination on the papilla and the first rugae. No such effect was evident for the second rugae. However, further studies with appropriate methodology are needed to validate this claim and solve the existing controversy in the literature. A limitation of the existing studies that use only medial and lateral rugae points to measure changes is that they assess only the relation between the limits of the rugae to each other and not the position of these anatomical structures within the mouth or the head. Furthermore, a limitation of superimposition studies that do not assess incisor movement in individual basis is that the results might be confounded by varying incisor movements in different patients.

A limitation of our study is that the registration of a 3D dental cast on a 2D cephalometric radiograph can involve errors attributed to the inherent limitations of the representation of a 3D object in a 2D image. The use of 3D radiographs could provide better information, but the increased radiation exposure required for their acquisition would not be justified in this patient group. Furthermore, the landmark identification process and the manual best fit of serial cephalometric radiographs when performing a maxillary structural superimposition,

might also involve errors. Here, the overall amount of landmark identification and superimposition error was satisfactory, considering that similar or higher amounts of error have been previously reported solely for the landmark identification process (24). Another limitation is that we measured the movement of only one central incisor, and thus, tested its association to the papilla and rugae changes. A more thorough approach could be to measure both central incisors and use the mean value as the testing variable. However, this was not possible, since usually one incisor was clearly visualised in the cephalometric radiograph in each case. Finally, we tested a sample with certain predefined characteristics, which adds precision to the outcomes. However, this affects generalisability of the results to other patient groups. Thus, the present results are applicable to growing patients with mild to moderate malocclusions, similar to those tested here. Further studies are needed to confirm these findings in other patient groups of different malocclusion, treatment, and growth status.

Conclusion

In the current sample, no significant differences were detected among the mean anteroposterior and vertical movements of all rugae points and the papilla point over time. However, the papilla and the first rugae points were affected by anterior tooth movement. Thus, their use to assess tooth movement cannot be recommended. These findings suggest that in similar patient groups, both the second and third rugae area can be used as superimposition reference, offering a larger surface that produces more robust outcomes (less sensitive to artifacts).

Furthermore, according to the study findings, the outcomes of a palatal rugae superimposition are comparable to those of a maxillary skeletal superimposition regarding the anteroposterior, but not the vertical dimension, where rugae movement over time should be considered.

Competing interests

The authors declare that they have no competing interests.

Funding

No funding was received.

Authors' contributions

NG and CP conducted retrospective sample selection and/or data generation. NG and CP had a substantial contribution to the preparation of the manuscript. NG and CP drafted and revised the manuscript. NG supervised the study. NG coordinated the preparation of the manuscript, and performed the statistical analysis. All authors read and approved the final manuscript.

References

1. Vasilakos G, Koniaris A, Wolf M, Halazonetis D, Gkantidis N. Early anterior crossbite correction through posterior bite opening: a 3D superimposition prospective cohort study. *Eur J Orthod.* 2018;40:364-371.
2. Björk A, Skieller V. Growth of the maxilla in three dimensions as revealed radiographically by the implant method. *Br J Orthod*. 1977;4:53-64.
3. Halazonetis DJ. From 2-dimensional cephalograms to 3-dimensional computed tomography scans. *Am J Orthod Dentofacial Orthop*. 2005;127:627–637
4. Gkantidis N, Schauseil M, Pazera P, Zorkun B, Katsaros C, Ludwig B. Evaluation of 3-dimensional superimposition techniques on various skeletal structures of the head using surface models. *PLoS One*. 2015;10:e0118810. doi: 10.1371/journal.pone.0118810
5. Friedli L, Kloukos D, Kanavakis G, Halazonetis D, Gkantidis N. The effect of threshold level on bone segmentation of cranial base structures from CT and CBCT images. *Sci Rep*. 2020;10:7361. doi: 10.1038/s41598-020-64383-9.
6. Stucki S, Gkantidis N. Assessment of techniques used for superimposition of maxillary and mandibular 3D surface models to evaluate tooth movement: a systematic review. *Eur J Orthod*. 2020;42:559-570. doi: 10.1093/ejo/cjz075.
7. Winkler J and Gkantidis N. Trueness and precision of intraoral scanners in the maxillary dental arch: an in vivo analysis. *Sci Rep*. 2020;10:1172. doi: 10.1038/s41598-020-58075-7.
8. Henninger E, Vasilakos G, Halazonetis D, Gkantidis N. The effect of regular dental cast artifacts on the 3D superimpositions of serial digital maxillary dental models. *Sci Rep*. 2019;9:10501. doi: 10.1038/s41598-019-46887-1
9. Mai DD, Stucki S, Gkantidis N. Assessment of methods used for 3-dimensional superimposition of craniofacial skeletal structures: a systematic review. *PeerJ*. 2020;8:e9263. doi:10.7717/peerj.9263
10. Vasilakos G, Schilling R, Halazonetis D, Gkantidis N. Assessment of different techniques for 3D superimposition of serial digital maxillary dental casts on palatal structures. *Sci Rep*. 2017;7:5838. doi: 10.1038/s41598-017-06013-5.
11. Almeida MA, Phillips C, Kula K, Tulloch C. Stability of the palatal rugae as landmarks for analysis of dental casts. *Angle Orthod*. 1995;65:43-48.
12. Bailey LT, Esmailnejad A, Almeida MA. Stability of the palatal rugae as landmarks for analysis of dental casts in extraction and nonextraction cases. *Angle Orthod*. 1996;66:73–78.
13. Chen G, Chen S, Zhang XY, Jiang RP, Liu Y, Shi FH, Xu T M. Stable region for maxillary dental cast superimposition in adults, studied with the aid of stable miniscrews. *Orthod Craniofac Res*. 2011;14:70–79.
14. Christou P, Kiliaridis S. Vertical growth-related changes in the positions of palatal rugae and maxillary incisors. *Am J Orthod Dentofacial Orthop*. 2008;133:81–86.

15. Jang I, Tanaka M, Koga Y, Iijima S, Yozgatian JH, Cha BK, Yoshida N. A novel method for the assessment of three-dimensional tooth movement during orthodontic treatment. *Angle Orthod*. 2009;79:447–453.
16. Hoggan BR, Sadowsky C. The use of palatal rugae for the assessment of anteroposterior tooth movements. *Am J Orthod Dentofacial Orthop*. 2001;119:482–488.
17. Kim HK, Moon SC, Lee SJ, Park YS. Three-dimensional biometric study of palatine rugae in children with a mixed-model analysis: a 9-year longitudinal study. *Am J Orthod Dentofacial Orthop*. 2012;141:590–597.
18. Bland JM, Altman DG. Comparing methods of measurement: why plotting difference against standard method is misleading. *Lancet*. 1995;346:1085-1087.
19. Zelditch ML, Swiderski DL, Sheets HD. Geometric morphometrics for biologists: a primer. *Academic Press*. 2012;11-13.
20. Lim PF, Neo KH, Sitoh L, Yeo K L, Stokes A. Adaptation of finger-smoothed irreversible hydrocolloid to impression surfaces. *Int J Prosthodont*. 1995;8:117–121.
21. Chatzigianni A, Halazonetis DJ. Geometric morphometric evaluation of cervical vertebrae shape and its relationship to skeletal maturation. *Am J Orthod Dentofacial Orthop*. 2009;136:481.e1-483. doi:10.1016/j.ajodo.2009.04.017
22. Enlow DH, Hans MG. *Essentials of facial growth*. Philadelphia, PA: W.B. Saunders Company; 1996.
23. Damstra J, Mistry D, Cruz C, Ren Y. Antero-posterior and transverse changes in the positions of palatal rugae after rapid maxillary expansion. *Eur J Orthod*. 2009;31:327-332.
24. Chien PC, Parks ET, Eraso F, Hartsfield JK, Roberts WE, Ofner S. Comparison of reliability in anatomical landmark identification using two-dimensional digital cephalometrics and three-dimensional cone beam computed tomography in vivo. *Dentomaxillofac Radiol*. 2009;38:262-273.

Figure legends

Figure 1. A. Pre-treatment and B. post-treatment maxillary dental models showing the landmarks placed in the palate to depict the distal point of the incisive papilla (P0; red circle) and the midpoints of the first, second, and third rugae, starting from mesially towards distally (R1, R2, R3; purple circles).

Figure 2. A. Post-treatment cephalometric radiograph. B. Post-treatment maxillary dental cast, registered on the corresponding cephalometric radiograph to facilitate the placement of the papilla and rugae points. C. All reference planes, curves, and landmarks placed on the cephalometric radiograph for the needs of the study. Detailed description is provided in Supplementary Table 2.

Figure 3. A. Pre-treatment and B. post-treatment cephalometric radiographs digitized and adjusted to facilitate the maxillary structural superimposition. C. Superimposed pre-and post-treatment radiographs. Yellow color indicates overlap of corresponding anatomical structures.

Figure 4. A. Box plots showing the anteroposterior movement of the papilla and rugae points during treatment, measured following the maxillary structural or the Sella superimposition of serial radiographs. B. Box plots showing the vertical movement of the papilla and rugae points during treatment, measured following the maxillary structural superimposition of serial radiographs or superimposition on ANS-PNS plane. The upper limit of the black line represents the maximum value, the lower limit the minimum value, the box the interquartile range, and the horizontal line the median value. Outliers are shown as colored dots. P0: papilla point; R1, R2, R3: rugae points

Figure 5. Box plots showing the anteroposterior and vertical movement, as well as the change in inclination due to treatment, of a central maxillary incisor, measured according to the occlusal plane, following the maxillary structural superimposition. The upper limit of the black line represents the maximum value, the lower limit the minimum value, the box the interquartile range, and the horizontal line the median value.

Table legends

Table 1. Spearman's correlations of the incisor movements and inclinations with the movements of the papilla and rugae points.

Supplementary Table 1. Detailed description of the inclusion criteria used for the study.

1. European ancestry.
2. No congenital anomalies, syndromes, or systemic diseases that could affect craniofacial morphology and tooth movement.
3. Non-extraction orthodontic treatment with fixed appliances in both jaws.
4. Age when the pre-treatment records where obtained (T0): 10.0 - 13.5 years old.
5. Treatment duration between 1.5 and 3.5 years.
6. No appliance on the palate at least 1 year prior to T0 records and during treatment.
7. A minimum of 1 year after the end of any previous orthodontic treatment at T0.
8. A maximum of 6 months from the T0 to treatment start.
9. Early permanent dentition at T0 (1st molar to 1st molar fully erupted, not considering 2nd premolars)
10. No missing teeth from 2nd molar to 2nd molar.
11. No impacted or ectopically erupted canines.
12. No extreme craniofacial pattern at T0 as defined by the following cephalometric variables: a) 28° < GoGnSN < 36°, b) 4° < facial contour angle < 20°, and c) 1° < ANB < 7°.
13. Molar Class I or less than ½ cusp Class II at T0.
14. No extreme malocclusion indicated by: a) 1 < overbite < 6 mm, b) 1 < overjet < 6 mm, and c) 1 < crowding < 6 mm.
15. No severe posterior crossbite at T0 (> 3.5 mm total transversal discrepancy).
16. No large facial asymmetries inspected visually by two specialists.
17. No active expansion of dental arches, apart from that caused by the orthodontic wires.
18. Clinically acceptable occlusion at T1 (< 1/4 deviation from Class I).
19. Cephalometric radiographs of adequate quality (visual inspection), with a ruler to measure the magnification factor.
20. Cephalometric radiographs where both maxillary central incisors had similar position and inclination or where the right or left incisor was clearly visualized (visual inspection).

Supplementary Table 2. Description of the landmarks and curves used for the study.

Landmarks	**Abbreviations**	**Definitions**
Nasion	N	Midpoint of the frontonasal suture at the most anterior aspect.
Sella	S	Center of hypophyseal fossa (sella turcica).
Papilla	P0	Most distal point of the incisive papilla.
Pterygomaxillary fissure	PTM Structural	Point at the area of the pterygomaxillary fissure that was transferred from T0 to T1 radiograph, following maxillary structural superimposition.
Anterior nasal spine	ANS	Most anterior point of the maxilla.
Posterior nasal spine	PNS	Posterior hard-tissue limit of the palate.
Rugae 1	R1	Midpoint of the 1st rugae, defined as the most anterior rugae.
Rugae 2	R2	Midpoint of the 2nd rugae, immediately posterior to the 1st rugae.
Rugae 3	R3	Midpoint of the 3rd rugae, posterior to the 2nd rugae.
Anterior occlusal		Point placed anteriorly to facilitate drawing of the occlusal plane.
Posterior occlusal		Point placed posteriorly to facilitate drawing of the occlusal plane.
Apex of the maxillary central incisor	U1 apex	Apex of a specific central incisor, that was predefined to be easily identified in the cephalometric radiograph.
Tip of the maxillary central incisor	U1 tip	Lowest point on the incisal edge of a specific central incisor, that was predefined to be easily identified in the cephalometric radiograph.
Centroid of the maxillary central incisor	-	Point at the center of the anatomical crown of a specific central incisor, that was predefined to be easily identified in the cephalometric radiograph.
Curves	**Abbreviations**	**Definitions**
Zygomatic maxillary curve	-	Curve delineating the contour of the middle part of the anterior zygomatic process of the maxilla. The anterior wall of the process was used as a reference for the structural superimposition.
U1 crown curve	-	Crown of a specific central incisor, that was predefined to be easily identified in the cephalometric radiograph.

Supplementary Table 3. Measurement error based on duplicated measurements performed on 10 subjects.

	Original values		Absolute values	
	Median	Range	Median	Range
U1 to occlusal plane, Vertical mov.	0.10	-0.90, 1.40	0.50	0.00, 1.40
U1 to occlusal plane, Horizontal mov.	-0.35	-1.30, 1.30	0.50	0.00, 1.30
U1, Inclination	0.30	-1.00, 1.60	0.40	0.10, 1.60
P0 to ANS-PNS, Vertical mov.	0.20	-0.80, 0.50	0.30	0.00, 0.80
R1 to ANS-PNS, Vertical mov.	0.15	-0.90, 1.20	0.35	0.00, 1.20
R2 to ANS-PNS, Vertical mov.	-0.10	-0.40, 0.60	0.25	0.00, 0.60
R3 to ANS-PNS, Vertical mov.	0.05	-0.40, 1.00	0.20	0.00, 1.00
P0 to PTM (vertical to ANS-PNS), Vertical mov.	-0.20	-1.40, 1.50	0.45	0.00, 1.50
R1 to PTM (vertical to ANS-PNS), Vertical mov.	0.05	-1.10, 1.70	0.70	0.30, 1.70
R2 to PTM (vertical to ANS-PNS), Vertical mov.	-0.50	-1.20, 1.20	0.90	0.30, 1.20
R3 to PTM (vertical to ANS-PNS), Vertical mov.	-0.20	-0.90, 1.70	0.60	0.10, 1.70
P0 to PTM (vertical to ANS-PNS), Horizontal mov.	0.10	-0.90, 0.80	0.30	0.10, 0.90
R1 to PTM (vertical to ANS-PNS), Horizontal mov.	-0.10	-0.60, 0.80	0.40	0.00, 0.80
R2 to PTM (vertical to ANS-PNS), Horizontal mov.	-0.15	-0.90, 1.10	0.40	0.00, 1.10
R3 to PTM (vertical to ANS-PNS), Horizontal mov.	0.00	-0.60, 1.10	0.25	0.00, 1.10
P0 to Sella (vertical to ANS-PNS), Horizontal mov.	0.05	-0.20, 0.90	0.20	0.00, 0.90
R1 to Sella (vertical to ANS-PNS), Horizontal mov.	0.10	-0.40, 0.40	0.15	0.00, 0.40
R2 to Sella (vertical to ANS-PNS), Horizontal mov.	0.00	-0.40, 0.50	0.30	0.00, 0.50
R3 to Sella (vertical to ANS-PNS), Horizontal mov.	0.15	-0.60, 0.60	0.25	0.10, 0.60

mov.: movement

Supplementary Figure 1. Scatter plots showing the relevant data to the correlations reported at Table 2 and had p < 0.10. The dashed line shows the least squares linear line that best fits the data. Movements are presented in millimeters and inclinations in degrees. P0: papilla point; R1, R2, R3: rugae points